E. Moghimirad, J. Bamber, E. Harris (2018) Dynamic contrast enhanced ultrasound imaging; the effect of imaging modes and parameter settings for a microvascular phantom. in: Proc 2018 IEEE International Ultrasonics Symposium, Oct. 22-25, 2018, Kobe, Japan. INSPEC Accession Number: (tbc). Electronic ISSN: 1948-5727. doi: 10.1109/ULTSYM.2018.tbc. (http://ieeexplore.ieee.org/document/tbc/). (in press)

Dynamic contrast enhanced ultrasound imaging; the effect of imaging modes and parameter settings for a microvascular phantom

Elahe Moghimirad*†, Jeffrey Bamber*, Emma Harris*
*Joint Department of Physics and CRUK Cancer Imaging Centre,
The Institute of Cancer Research and Royal Marsden NHS Foundation Trust, Sutton, London, United Kingdom
† elahe.moghimirad@icr.ac.uk, elahe.moghimirad@gmail.com

***Abstract*—Dynamic contrast enhanced ultrasound (DCE-US) imaging has the potential to provide quantitative information which is sensitive to tumour perfusion, an indicator for tumour response to radiotherapy. To increase the reproducibility of time-intensity curve (TIC) characteristics, we are developing a 3D DCE-US imaging system. There are, however, many choices to be made in system design, such as whether to use plane wave (PWI) or focused imaging (FI), and the values to use for parameters such as focal depth (FD), F-number (F#), mechanical index (MI) and number of angles (NA) (for PWI). We evaluated the effect of such choices on TICs (we refer to time-amplitude curve (TAC) here), using a microvascular flow phantom containing ∼100,000 parallel microtubes, each 200 μm in diameter. DCE-US 2D images were obtained using a Vantage (Verasonics Inc.) and a pulse-inversion algorithm. 800 frames were recorded at 10 Hz for PWI and FI. All measurements were repeated 3 times, injecting 0.4 ml of contrast agent (Sonozoid) and changing one parameter at a time, using the values: FD = 20, 40 mm; F# = 2, 4; MI = 0.11, 0.15, 0.25; NA = 3, 7, 11. For a large region of interest which included the periphery of the phantom, TACs were sharp and single-peaked for F2 but broader and double-peaked for F4, consistent with F4 averaging over a greater focal volume than F2. Choosing a smaller more central ROI reduced the effect but did not eliminate it completely. Placing the focus deeper than the center reduced the TAC amplitude due to attenuation but also resulted in a flatter TAC. PWI amplitude was greatest for 3 angles with evidence that this may be due to side lobe artefacts added to the contrast signal. TAC characteristics are thus expected to be highly sensitive to imaging parameters. This should be considered in longitudinal studies.**

***Index Terms*—Dynamic contrast enhanced ultrasound imaging, time intensity curve (TIC), time amplitude curve (TAC), imaging mode, parameter setting, microvascular phantom.**

I. Introduction

Chemoradiation can significantly affect tumour blood perfusion soon after treatment, which can be used as an indicator to differentiate between responders and non-responders [1], [2]. On the other hand, standard evaluation of tumour response based on the tumour size usually needs one to two months of treatment before it shows any meaningful changes. Therefore, an accurate and reproducible technique to assess changes in aspects of tumour function, such as vascularity, at early time points, i.e. within one to two weeks, may be vital as a potential way to improve how we treat patients [3]. Dynamic contrast enhanced ultrasound (DCE-US) imaging provides perfusion information [4] and has been recognized as a useful tool to assess tumour response. This is based on the change in contrast signal of the region of interest (ROI), known as a time-intensity curve (TIC), when microbubbles pass through the region [5]. Changes in TIC characteristics such as wash-in time, wash-out time and peak intensity have been related to the function of tumour vasculature and thus its response to chemoradiotherapy [1], [2]. To make a reliable assessment of these characteristics specially in longitudinal studies, an accurate, precise and reproducible quantification technique is needed, ideally irrespective of the ultrasound equipment, imaging mode, system parameters and subject variables. Considering this, we are developing a 3D DCE-US imaging system, which is expected to increase reproducibility of the measured contrast ultrasound characteristics between imaging sessions compared to 2D, thereby improving sensitivity to therapy-induced changes in the vasculature [6]–[11]. There are, however, many choices to be made in system design, such as whether to use plane wave imaging (PWI) or focused imaging (FI), and the values to use for parameters such as focal depth (FD), F-number (F#), mechanical index (MI) and number of angles (NA) (for PWI). Most of the previous studies on TIC evaluation have focused on scanner parameters such as dynamic range and gain, compression, TIC fitting or region of interest (ROI) selection [12]–[15]. Some groups have studied contrast enhanced ultrasound imaging (CEUS) variability with respect to one or two system parameters including pulse length, frequency, MI and imaging modes [16]–[18], without further evaluation of the corresponding TICs. Here we evaluate the effect of such choices on TICs for a microvascular flow phantom *in vitro*. Since contrast echo amplitude images were analysed in the present work, from hereon we refer to time-amplitude curves (TACs) rather than TICs.

This work is supported by Cancer Research UK Program C20892/A23557.

II. Materials and Methods

A dialysis cartridge was used as the microvasculature phantom, containing ∼100,000 parallel microtubes, each 200 μm in diameter. It was connected to a peristaltic pump (HR flow inducer type MHRE 200-250v, Watson Marlowe Ltd, Falmouth, UK) as shown in fig. 1. Maintaining a constant flow of degassed water through the system, 0.4 ml of contrast agent

(SonozoidTM; GE Healthcare, Oslo, Norway) was injected at 3.18 ml/min as a bolus injection using a NE-1010 injection pump (New Era Pump Systems Inc., NY, USA). DCE-US images were obtained using a Vantage^{TM} system (Verasonics Inc., Kirkland WA, USA) and reconstructed using a two-pulse pulse-inversion algorithm with 150 μs pulse intervals to generate a microbubble-specific echo signal [19]. To evaluate the TACs, 850 frames were acquired for both FI and PWI, corresponding to 85 seconds of TAC starting from injection, which spanned the full wash-in and a part of wash-out period. For each selected ROI, TAC was calculated as the mean signal amplitude of the ROI pixels. 128 focused beamlines were acquired for FI with 300 μs (= 2 $\times$ pulse interval) line intervals and 10 Hz image frame rate. For PWI, frame rate was also adjusted to 10 Hz with the compounding angle intervals of 300 μs. Various number of compounding angles were used for PWI tilted from -10 to +10 degrees. Default parameters were selected so that FI and PWI had similar contrast and microbubble disruption rate in a simple single-vessel flow phantom. The parameters were: FD = 20 mm (for FI), F# = 4, MI = 0.15, transmit frequency = 4 MHz, NA = 7 (for PWI). To evaluate the TAC for each parameter independent of the others, measurements were repeated changing one parameter at a time, using the values: FD = 20 mm, 40 mm; F# = 2, 4; MI = 0.11, 0.15, 0.25; NA = 3, 7, 11. All measurements were repeated 3 times. TACs were then evaluated for FI and PWI for different ROIs.

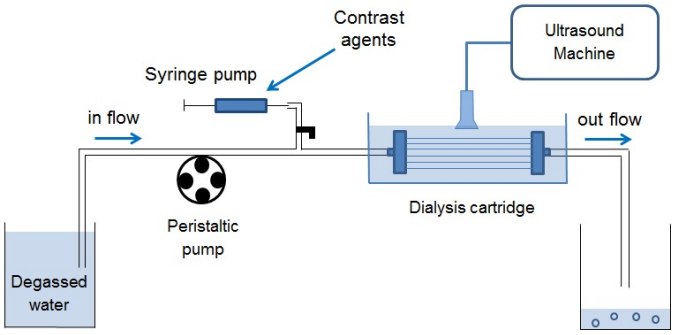

Fig. 1: Phantom setup composed of a dialysis cartridge connected to a peristaltic pump and an injection pump to inject the contrast agent through the system. (The mixed fluid of water and contrast agent was removed from the system after passing through the cartridge.)

III. Results

Fig. 2a shows the FI Bmode (left) and contrast mode (right) images of the phantom in absence of the contrast agent. The phantom provided reproducible TACs that were tumour-like in being dependent on distance from the center. Blue, red and green ROIs correspond to a big ROI (ROI-big), a small central one (ROI-center) and a peripheral one (ROI-periphery), respectively. Fig. 2b and 2c show TACs for FI and PWI for different ROIs in matching colours. For both FI and PWI, TACs had 2 peaks for all ROIs and the peripheral ROI (in green) gave a slower wash-in compared to the central ROI TAC (in red). PWI had a smoother TACs with less distinct peaks compared to the FI TACs. Also, the peak amplitudes were greater for FI.

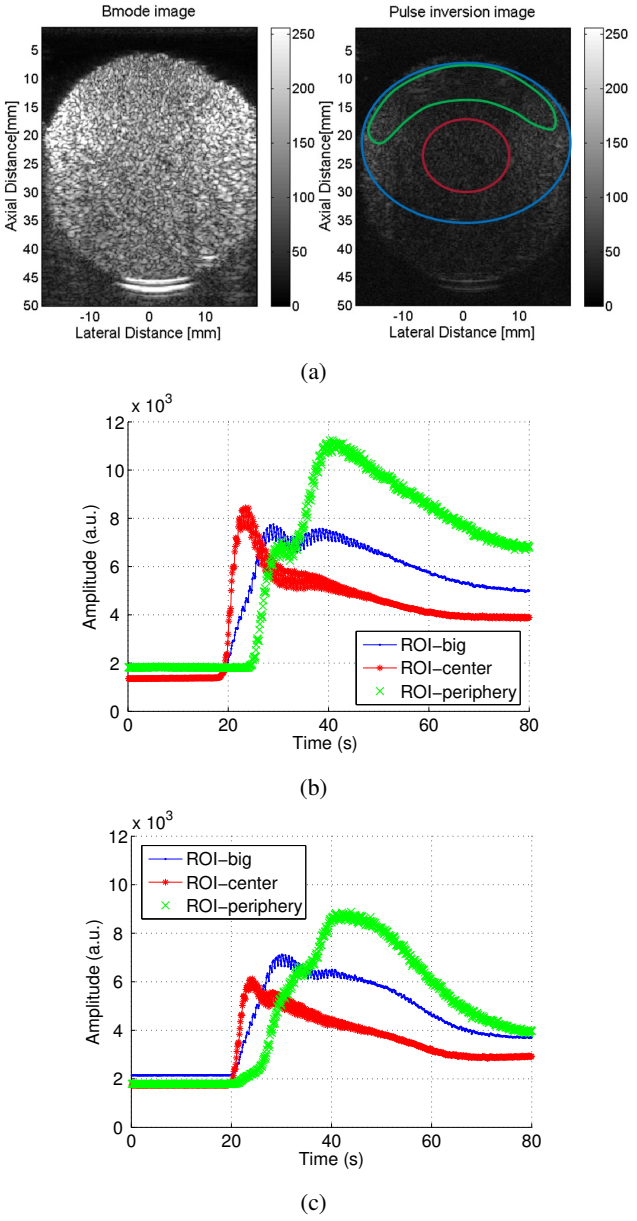

Fig. 2: (a) Bmode (left) and contrast mode (right) of the phantom. Blue, red and green ROIs correspond to ROI-big, ROI-center and ROI-periphery in (b) and (c), (b) FI TACs for different ROIs and (c) PWI TACs for different ROIs.

Fig. 3 shows FI TACs for different F#s and FDs using ROI-big (fig. 3a) and ROI-center (fig. 3b). They show that for ROI-big, TACs were sharp and single-peaked for F2 but broader and double-peaked for F4 (fig. 3a). Choosing a smaller ROI reduced the second peak for F4 but did not eliminate it completely (fig. 3b). Placing the focus deeper than the center reduced the TAC amplitude (green) for both ROIs due to

attenuation but also resulted in less region dependence and a flatter TAC.

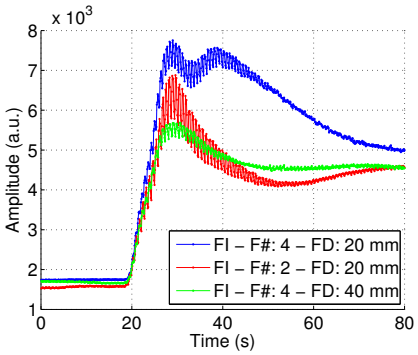

(a)

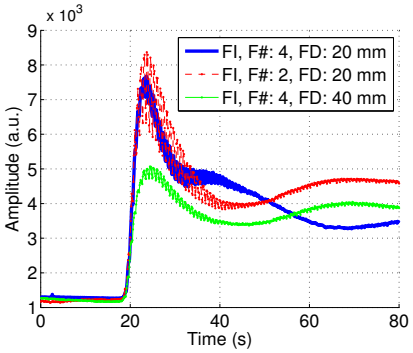

(b)

Fig. 3: FI TACs for different F#s and FDs using (a) ROI-big and (b) ROI-center.

PWI TAC amplitude was greatest for 3 angles (fig. 4) and reduced with increasing numbers of angles. Higher MIs gave greater TAC amplitudes for both PWI and FI as expected. Unlike 0.1 and 0.15 MI where FI and PWI had similar TAC amplitudes, at 0.25 MI, FI had greater amplitude compared to PWI (fig. 5).

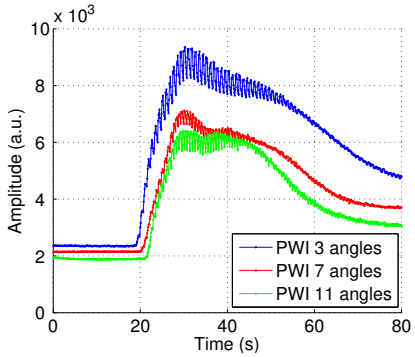

Fig. 4: PWI TACs for different number of compounding angles.

IV. Discussion

The two-peaked appearance of the TACs were likely caused by the combination of two distinct wash-in phases, one faster

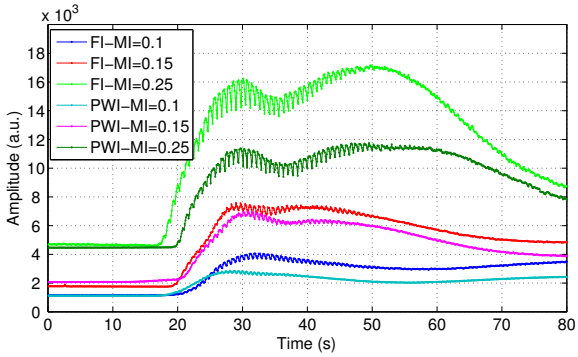

Fig. 5: FI and PWI TACs for different MIs.

than the other (fig. 2b and 2c). The phantom had a spatially heterogeneous wash-in pattern; the contrast agent arrived at the center first and then at the periphery. Therefore a faster wash-in in the central ROI compared to the peripheral ROI was expected, see fig. 2b. The largest ROI, ROI-big, which contained both periphery and central areas, may have a combined pattern of these two ROIs, and so there was no dominant peak in the blue curves (see fig. 2b and 2c).

The main difference between FI and PWI TACs was that PWI gave smoother TACs. This was probably caused by three different phenomena. 1) PWI has a wider lateral beam width which in combination with forward scattering (rescattering) of the contrast echo signal, can result in depth confusion in the TACs. This means that each ROI may contain information that is a combination of signal from its own pixels and forward scattered signal from the shallower (anterior) region of the phantom. The impact of forward scattering mostly depends on the shape and the width of the beam around and anterior to the ROI. 2) Target (microbubbles) movement between the compunding angles, can lead to failure of synthetic focusing for PWI and as a result a wider point spread function (PSF) and a greater sidelobes, which can lead to a combination of information from different areas and a smoother TAC. 3) It may be partially due to high frequency grating lobe artefacts which we observed in a separate study where PWI and FI were evaluated over a single vessel flow phantom (not shown here) and PWI was seen to suffer from grating lobe artefacts that originated from high frequency component of the contrast signal (not seen for FI). Grating lobes usually have a greater footprint than the mainlobe and can mix the information from different areas and depths which in this case, probably led to a smoother TAC with less distinct peaks for PWI.

For ROI-big, TACs were sharp and single-peaked for F2 but broader and double-peaked for F4 (fig. 3a). Choosing a smaller more central ROI, reduced the second peak amplitude for F4 but did not eliminate it completely (fig. 3b). It is likely that because F4 provides a weaker focus, it may be more influenced by the forward scattering coming from anterior pixels. As mentioned above, the effect of forward scattering and depth confusion depends on the shape and width of the beam around and anterior to a particular pixel. It was also observed that TAC

for F2 was only localized around the focal region and moving the ROI away from the focal depth towards the periphery, TAC for F2 was broader compared to F4 (not shown here). This is probably because F2 has a wider lateral beam width out of the focal region compared to F4 which can increase the forward scattering effect for F2. It should be noted that as the microtubes were not wall-less, the scattering nature of them may add to the forward scattering effect compared to an in-vivo situation which should be examined in future works.

Tumours are usually similar to this phantom in terms of heterogeneity [20], however, the contrast agents tend to wash in to the periphery of the tumour first, the reverse to our phantom. Therefore, the same problems are expected to be seen in-vivo. For a small ROI at the focal region or a small tumour in general ($<$10 mm diameter), FI with a tight focus (small F#) seems to be the best choice to provide a localized TAC, however, for larger tumours, if out of focus regions are also being considered, small F#'s gives a broad and smoothed TAC for that regions. For larger tumours with multiple in and out of focus ROIs or a big ROI in general, it might be better to use larger F# which provides more homogeneous TACs, although this will be a combination of the ROI pixels signal and the forward scattered signal from anterior pixels. This also happens for PWI to a much greater extent. Multi-focal FI with low F#'s may solve the problem at the expense of temporal resolution which may present a problem for 3D imaging. So, there are trade-offs in choosing the best setting and the decision should be made based on the application.

PWI TAC amplitude was greatest for 3 angles (fig. 4). This may be due to side lobe and high frequency artefacts added to the contrast signal, which were observed in the image (data not shown).

TAC for different MI's showed that, unlike 0.1 and 0.15 MI where FI and PWI gave similar TAC amplitudes, at 0.25 MI, FI has a greater amplitude compared to PWI (fig. 5). A likely cause is that at higher MIs, microbubble disruption rate increases which then can lead to incoherent summation between the PWI compounding angles and reduce the PWI amplitude. On the other hand, the higher desruption rate between the PI positive and negative pulses can lead to a false contrast increase for FI and PWI. The combination of the two phenomena would result in a greater amplitude for FI compared to PWI at higher MIs.

V. Conclusion

This study showed that TAC characteristics are highly sensitive to imaging parameters and this should be considered in longitudinal studies. Also, the parameter setting should be carefully selected base on the tumour and ROI size. FI with smaller F# is a good option for small tumours/ROIs, however, this study suggest that bigger F#'s give a more homogeneous TAC's in larger tumours/ROIs. PWI imaging suffered a greater amount of depth confusion in this study and provided a smoothed TAC. Evaluating different pulse shapes or aperture sizes to reduce these effects is a topic for future work.

References

[1] G. Nishimura, K. Yabuki, M. Hata, M. Komatsu, T. Taguchi, M. Takahashi, O. Shiono, D. Sano, Y. Arai, H. Takahashi, Y. Chiba, and N. Oridate, "Imaging strategy for response evaluation to chemoradiotherapy of the nodal disease in patients with head and neck squamous cell carcinoma," *Int J of clinical oncol*, vol. 21, pp. 658–667, 2016.

[2] K. Tawada, T. Yamaguchi, A. Kobayashi, T. Ishihara, K. Sudo, K. Nakamura, T. Hara, T. Denda, M. Matsuyama, and O. Yokosuka, "Changes in tumor vascularity depicted by contrast-enhanced ultrasonography as a predictor of chemotherapeutic effect in patients with unresectable pancreatic cancer," *Pancreas*, vol. 38, pp. 30–35, 2009.

[3] G. C. Jayson, R. Kerbel, L. M. Ellis, and A. L. Harris, "Antiangiogenic therapy in oncology: current status and future directions," *The Lancet*, vol. 388, pp. 518–529, 2016.

[4] J. Y. Lu, J. Cheng, and J. Wang, "High frame rate imaging system for limited diffraction array beam imaging with square-wave aperture weightings," *IEEE Trans. Ultrason., Ferroelec., Freq. Contr.*, vol. 53, pp. 1796–1812, 2006.

[5] A. Fleischer, K. Niermann, E. Donnelly, T. Yankeelov, K. Canniff, D. Hallahan, and M. Rothenberg, "Sonographic depiction of microvessel perfusion," *J Ultrasound Med.*, vol. 11, pp. 1499–506, 2004.

[6] H. Wang, O. Kaneko, L. Tian, D. Hristov, and J. K. Willmann, "Three-dimensional ultrasound molecular imaging of angiogenesis in colon cancer using a clinical matrix array ultrasound transducer," *Invest radiology*, vol. 50, pp. 322–329, 2015.

[7] J. B. Liu, G. Wansaicheong, D. A. Merton, F. Forsberg, and B. B. Goldberg, "Contrast-enhanced ultrasound imaging: State of the art," *J Med Ultrasound*, vol. 13, pp. 109–126, 2005.

[8] K. Hoyt, A. Sorace, and R. Saini, "Quantitative mapping of tumor vascularity using volumetric contrast enhanced ultrasound," *Invest Radiol.*, vol. 47, pp. 167–174, 2012.

[9] ——, "Volumetric contrast-enhanced ultrasound imaging to assess early response to apoptosis-inducing antideath receptor 5 antibody therapy in a breast cancer animal model," *J Ultrasound Med*, vol. 31, pp. 1759–1766, 2012.

[10] M. Mahoney, A. Sorace, J. Warram, S. Samuel, and K. Hoyt, "Volumetric contrast-enhanced ultrasound imaging of renal perfusion," *J Ultrasound Med*, vol. 33, pp. 1427–1437, 2014.

[11] S. Feingold, R. Gessner, I. M. Guracar, and P. A. Dayton, "Quantitative volumetric perfusion mapping of the microvasculature using contrast ultrasound," *Invest Radiol*, vol. 45, pp. 669–74, 2010.

[12] M. X. Tang, H. Mulvana, T. Gauthier, A. K. P. Lim, D. O. Cosgrove, R. J. Eckersley, and E. Stride, "Quantitative contrast-enhanced ultrasound imaging: a review of sources of variability," *Interface Focus*, vol. 1, pp. 520–539, 2011.

[13] T. P. Gauthier, M. A. Averkiou, and E. L. S. Leen, "Perfusion quantification using dynamic contrast-enhanced ultrasound: The impact of dynamic range and gain on timeintensity curves," *Ultrasonics, Elsevier*, vol. 51, pp. 102–106, 2011.

[14] A. Ignee, M. Jedrejczyk, G. Schuessler, W. Jakubowski, and C. F. Dietrich, "Quantitative contrast enhanced ultrasound of the liver for time intensity curvesreliability and potential sources of errors," *Europ. J of Radio., Elsevier*, vol. 73, pp. 153–158, 2010.

[15] O. Lucidarme, J. M. Correas, and S. L. Bridal, "Blood flow quantification with contrast-enhanced us: Entrance in the section phenomenon-phantom and rabbit study," *Radiolog*, vol. 228, pp. 473–479, 2003.

[16] J. Viti, H. J. Vos, N. de Jong, F. Guidi, and P. Tortoli, "Detection of contrast agents: Plane wave versus focused transmission," *Trans. Ultrason., Ferroelec., Freq. Contr.*, vol. 63, pp. 2676–2683, 2016.

[17] O. Couture, M. Fink, and M. Tanter, "Ultrasound contrast plane wave imaging," *Trans. Ultrason., Ferroelec., Freq. Contr.*, vol. 59, pp. 2676–2683, 2012.

[18] N. R. Vaka, "Comparison and optimization of insonation strategies for contrast enhanced ultrasound imaging." Ph.D. dissertation, Linkoping University, 2011.

[19] D. H. Simpson, C. T. Chin, and P. N. Burns, "Pulse inversion doppler: A new method for detecting nonlinear echoes from microbubble contrast agents," *IEEE Trans. Ultrason., Ferroelec., Freq. Contr.*, vol. 46, pp. 372–382, 1999.

[20] R. J. Gillies, P. A. Schornack, T. W. Secomb, and N. Raghunand, "Causes and effects of heterogeneous perfusion in tumours," *Neoplasia*, vol. 1, pp. 197–207, 1999.